A PRELIMINARY INVESTIGATION OF HEAT TRANSFER BY BUBBLES IN AN AIR-WATER SYSTEM

12T

A THESIS

Presented to

the Faculty of the Graduate Division

Georgia Institute of Technology

In Partial Fulfillment

of the Requirements for the Degree

Master of Science in Chemical Engineering

By

Frank Augustian Morgan

June 1954

"In presenting the dissertation as a partial fulfillment of the requirements for an advanced degree from the Georgia Institute of Technology, I agree that the Library of the Institution shall make it available for inspection and circulation in accordance with its regulations governing materials of this type. I agree that permission to copy from, or to publish from, this dissertation may be granted by the professor under whose direction it was written, or such copying or publication is solely for scholarly purposes and does not involve potential financial gain. It is understood that any copying from, or publication of, this dissertation which involves potential financial gain will not be allowed without written permission.

_____

_____"

A PRELIMINARY INVESTIGATION OF HEAT TRANSFER BY BUBBLES IN AN AIR-WATER SYSTEM

By

Frank Augustian Morgan

APPROVED

Date of Approval June 4, 1954

ACKNOWLEDGMENT

The author wishes to express his heartfelt thanks to Dr. H. V. Grubb for his many valuable suggestions and continual encouragement throughout the progress of the investigation.

TABLE OF CONTENTS

LIST OF TABLES

LIST OF ILLUSTRATIONS

A PRELIMINARY INVESTIGATION OF HEAT TRANSFER BY BUBBLES IN AN AIR-WATER SYSTEM

SUMMARY

The purpose of the problem was to determine the heat transfer coefficients of air bubbles rising through water at a temperature higher than that of the entering air.

A porous ceramic plate and a sintered glass plate inserted in a lucite column were used to produce the bubbles which were studied. High speed photography was utilized to determine the size and number of bubbles necessary for the calculation of area available for heat transfer. Temperature measurements of the entering and exit water, coupled with temperature and humidity measurement of the entering and exit air completed the data necessary for calculating heat transfer coefficients. Two slightly different methods of calculation of heat transfer coefficients were used because of modification of experimental procedure. The coefficients calculated when the ceramic plate was being used were based on data taken at one instant of time after equilibrium has been reached. Data were taken over a period of time, usually twenty-five to thirty minutes, when the sintered glass plate was used, and calculation of heat transfer coefficients involved graphical integration of the data. Results derived from both methods agreed rather well in order of magnitude.

The results showed the coefficients of such heat transfer to be relatively low as compared to other methods of transferring heat to air. It was also shown that these coefficients were affected by flow rates which, in turn, affected bubble size and terminal rising velocity of the bubbles. No quantitative statement was formulated to show the relation of these variables to the heat transfer coefficients, due to the limited range of experimental data which were taken. The graphical presentations of the results do, however, indicate the trend of the effect of the experimental variables and point the way for future study of the subject. With reference to future study, it is recommended that experimental work be carried out on a larger scale than that of this investigation in order to reduce the effect of errors made in temperature and flow rate measurements. It would also be desirable to study other gas-liquid systems and develop methods of predicting heat transfer coefficients for any gas-liquid system.

CHAPTER I

INTRODUCTION

The purpose of this investigation was to determine the rate of heat transfer between a heated liquid and gas bubbles rising through the liquid. The study was limited to an air-water system. An effort was made to determine the effect of the bubble size and the mass flow rate of the gas upon the coefficient of heat transfer. The practical application of this study is limited at the present time, although the role of gas bubbles is an important one in many physical and chemical processes involving interaction between gaseous and liquid systems.

The large number of variables which affect heat transfer in such a case add greatly to the complexity of the problem, and, consequently, little previous work is reported in the literature on this particular phase of heat transfer. Many studies have been made on the effect of bubble formation in boiling heat transfer (1), but there is little similarity between boiling heat transfer and the subject of this investigation. A study of the articles on boiling heat transfer reveals, however, that little is known about the actual mechanism of heat transfer to a bubble.

The lack of previous work on the subject has greatly limited the opportunity for correlating the results of other

investigations with the results of this investigation. It is hoped that this study will stimulate interest and lead to other investigations of the basic mechanism of heat transfer through gas bubbles so that methods of predicting transfer coefficients for other systems will be developed.

CHAPTER II

EQUIPMENT AND PROCEDURE

The major items of equipment used in the experimental work were a constant temperature bath, an electric hygrometer manufactured by the American Instrument Company, Silver Springs, Maryland; a three-foot vertical lucite column two and one-quarter inches in diameter, a cylinder of compressed air, a Speedgraphic camera with strobescopic light attachment, and a 1/4 h.p. centrifugal pump. Other items employed were mercury thermometers, rotameters, heaters, stirrers, reducing valves, mercury manometer, and the necessary connecting pipes and tubing. The schematic diagram of the experimental set-up is shown in Figure 1.

Two slightly different experimental set-ups were used which will be referred to as Set-up A and Set-up B. Set-up A will be described first as to arrangement of equipment and cycle of operation, and then the modifications resulting in Set-up B will be described.

Set-up A.--As the first step of the operation, the water in the constant-temperature bath was heated to a temperature of 46.8° C. using copper coil heaters and an electric stirrer. The temperature was controlled within limits of $\pm$ 0.1°C. by a "merc to merc" thermoregulator manufactured by the Precision

KEY:

1 Heater, Stirrer, and Thermostat Control
2 Constant Temperature Bath
3 Centrifugal Pump
4 Rotameter
5, 6,7,8 Thermometers
9 Column
10,11 Humidity Sensing Elements
12 Humidifying Flask
13 Humidity Indicator
14 Rotameter
15,16 Reducing Valves
17 Compressed Air Cylinder

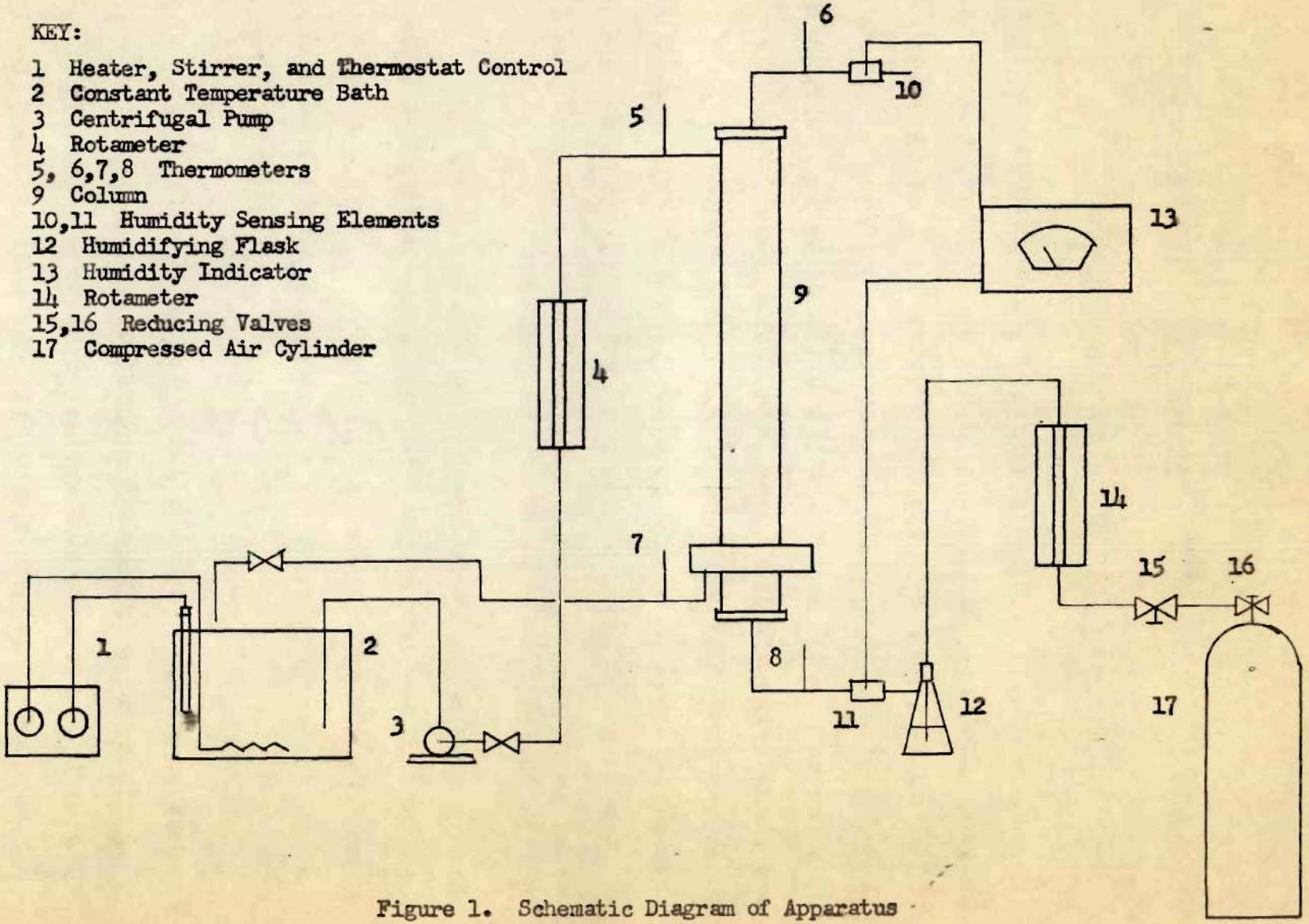

Figure 1. Schematic Diagram of Apparatus

Scientific Company. From the bath, the water was pumped by a small centrifugal pump through a rotameter to the top of the column. The rotameters used to measure the air and water flow rates were Tri-Flat rotameters, manufactured by the Fischer and Porter Company, Hatboro, Pennsylvania, especially for measuring low flow rates of gases and liquids. Immediately before entering the column, the water temperature was measured by a thermometer inserted in the line. All thermometers used were of the Anschuetz type graduated in 0.2° C. intervals from 0° to 55° C. and calibrated against a thermometer calibrated by the United States Bureau of Standards. After the water passed through the column, it was recirculated to the constant-temperature bath by gravity flow through a manifold at the base of the column. Its exit temperature was measured by a thermometer placed as near as possible to the outlet of the manifold. This completed the water cycle.

The air was supplied from a cylinder of compressed air containing 240 standard cubic feet initially under a pressure of 2200 lbs./in^2. It passed through two reducing valves in series being reduced from 2200 lbs./in.^{2} to 16 lbs./in.^{2}. After pressure reduction, the flow rate was measured by a Tri-Flat rotameter as it passed into a 1000 ml. flask containing water at room temperature. The air was admitted to the flask through a glass tube extending below the surface of the water almost to the bottom of the flask. As the air bubbled up

through the water to the surface, it became humidified to about 85-90 per cent of saturation. It then passed out through an outlet in the side of the flask to which was connected a piece of rubber tubing. Following the pre-humidification, the air flowed over an electric humidity sensing element which was housed in a three-inch section of a lucite tube and from there to the bottom of the water column previously described where the temperature was measured by a thermometer just before entering the column. Upon entering the column, the air passed up through a porous ceramic plug creating the bubbles that were to be studied. A pressure of 16 lbs./in.^{2} was found to be sufficient to keep the water from leaking through the plug and into the bottom section of the column where the air entered. The air bubbles passed up through the heated water in the column, being itself subsequently heated and humidified. As the bubbles broke free from the surface of the water at the top of the column, the heated air passed out through a port in the top of the column which was drilled and tapped for a 1/4-inch pipe. A thermometer was located in this line approximately three inches from the top of the column. Immediately following this thermometer was another humidity sensing element housed in the same manner as the previously mentioned element. The air was vented to the atmosphere after passing this humidity element.

The column itself was a three-foot section of lucite tubing of two inches inside diameter and two and one-quarter

inches outside diameter. The lucite tubing was chosen because of its low thermal conductivity, its machinability, its light weight, and its transparency.

The ceramic plug was inserted at the bottom of the column by machining the plug and counter-boring the column so that a close fit resulted. Another three-inch section of the lucite tube was similarly counter-bored, fitted and sealed to the bottom of the plug, making a continuous column with the plug located three inches from the bottom. Four equally spaced 10/32-inch holes were drilled around the circumference of the column one inch above the plug, and around these holes a circular lucite manifold was fitted and sealed to the column. A 1/4-inch hole was drilled and tapped in the bottom of the manifold through which the water returned to the constant temperature bath.

The purpose of the four water outlets at the base of the column was to lower the velocity of the water leaving any one outlet, thereby preventing bubbles from being swept out with the leaving water. This precaution, coupled with the low water rates which were used, eliminated this difficulty.

Two circular disks of lucite were drilled and tapped for 1/4-inch pipe and attached to the bottom and top of the column, completing the construction of the column.

To prevent excessive heat losses to the surroundings, the column was lagged with asbestos tape and one-inch preformed

corrugated asbestos insulation. Thermometer wells and adjoining pipes were also lagged with asbestos tape.

Calibration curves were furnished by the manufacturer for use with the rotameters for liquids with density of 1.0 gram per cubic centimeter and viscosity of 1.0 centipoise and air at 14.7 PSIA and 70^{0}F. Equations and graphs were also furnished with which to calibrate the instruments for use with liquids and gases at other conditions of density, temperature, and pressure. These calculations and calibrations were made for conditions of the experimental work and are shown in Figures 6 and 7 of the Appendix.

Difficulty was encountered with fluctuations of the air flow when only one pressure reducing valve was used, but this was satisfactorily eliminated by installing another manually operated valve and by keeping a close visual check on the rotameter float.

Humidity measurements were made with an electric hygrometer which measured per cent relative humidity. The sensing elements of the hygrometer could also be used to measure temperature of the air, and this method was used to measure the temperature of the inlet air in Set-up B. Calibration curves for this instrument were also furnished by the manufacturer and are shown in Figures 8, 9, and 10 of the Appendix.

Set-up B.--The second experimental set-up resembled the first with several exceptions. The water was not recirculated; instead, it was pumped into the column until it reached a height of 76 cm., and then the water was allowed to remain in the column until a run was completed.

The ceramic plug was also replaced by a sintered glass filter in order to obtain smaller and more uniform bubbles. The manifold was also removed, since the water was not re-circulated. Three ports were drilled in the column at the top, middle, and bottom, and in these, thermometers were inserted to measure the water temperature in the column.

A mercury manometer was inserted into the air line to indicate the air pressure after passing through the reducing valves. The entering air pressure was found to be approximately constant at 16.1 PSIA for all air flow rates in Set-ups A and B. This pressure was taken into account in calibration of the rotameter.

Procedure.--Two experimental procedures were used to obtain data, depending upon whether Set-up A or B was being used. The preliminary procedure was the same for both set-ups, the first step being the heating of the water to the desired temperature in the constant temperature bath. When this temperature was reached, the pump was started and water was circulated through the system. Simultaneously with the starting of the pump, the air valves were opened and air bubbled up

through the column. Fifteen minutes were generally allowed for the column and pipes to come to thermal equilibrium with the surroundings and with the water in the column. This was done to insure steady state conditions before the start of a run.

The actual run with Set-up A consisted of recording the inlet and exit temperature of the water and air and the inlet and exit humidity of the air and the flow rates of both water and air. Several runs using the same flow rates were generally made in succession, then the flow rates were changed and sufficient time was allowed for equilibrium to be reached before taking data for the next run. The water rates used were 0.208 lbs./min. and 0.408 lbs./min. and the air rates were 0.0746 lbs./hr., 0.151 lbs./hr., and 0.222 lbs./hr.

After the runs to collect data on temperature and flow rates were completed, the insulation was removed from the column so that pictures could be made. All of the conditions of the actual runs were duplicated as nearly as possible so that the photographs would be representative of the actual runs. Photographs were made with a Speedgraphic camera utilizing a strobescopic light of 1/2 milli-second duration for illumination. Close-ups were made of the center section of the column in order to obtain a picture of the average conditions of bubble size and turbulence in the column. Pictures were also made of the entire column to see if any coalescence was taking place and to check the uniformity of distribution of the bubbles through the length of the column.

In Set-up B, the water was not recirculated; therefore, no flow rates of the water were taken, but the height of the water was recorded. The change in the height of water with air in the column and with no air in the column was also recorded. The water temperature was taken as the average reading of the three thermometers inserted in the column, and the entering air temperature was measured with the humidity sensing element. The flow rate of air was recorded and maintained at a constant rate throughout a run which lasted from twenty to forty minutes with readings taken at five minute intervals. The same procedure as before was used for the photographic work.

CHAPTER III

THEORY

The data obtained from the experimental runs were used to calculate film coefficients for heat transfer from the water to the air bubbles. The coefficients which were calculated were based upon the estimated total surface area of bubbles in the column at any instant and the total sensible heat transferred to the air in a finite period of time; therefore, they would be more appropriately called overall heat transfer coefficients rather than coefficients for individual bubbles.

The basic equation for the calculation of these coefficients is expressed by the equation (1) where,

$$h = \frac{qs}{A(\Delta t)m} \qquad (1)$$

h = film coefficient, $\frac{BTU}{hr./ft^2/^oF}$

qs = sensible heat transferred $\frac{BTU}{hr.}$

A = total surface area of bubbles, ft^2

and $(\Delta t)m$ = log mean temperature difference, ^oF

The experimental set-up was similar to a countercurrent heat exchanger with cold air flowing up through the column countercurrent to hot water; therefore, the log mean temperature difference in equation (1) has the same significance as in the more general case of countercurrent exchangers.

The sensible heat transferred was calculated from the equation

$$qs = Gs_1(t_2-t_1) \tag{2}$$

where: G = flow rate of air, lbs./hr.

s_1 = heat capacity of entering air, $\frac{BTU}{lb./^oF}$

t_1 = temperature of entering air, ^oF

and t_2 = temperature of exit air, ^oF

The heat capacity of the entering air is the sum of the heat capacity of the dry air and water vapor which entered with it. This heat capacity was obtained from a humidity chart, the entering argument being the dry bulb temperature and the per cent relative humidity as measured by the electric hygrometer.

The area of equation (1) was based on the surface area of the bubbles given by equation (3) as follows:

$$A = n\pi D_b^2 \tag{3}$$

where: n = total number bubbles

and D_b = average bubble diameter, ft.

The average bubble diameter was determined from high speed photographs which were enlarged from two to three times actual size. The degree of enlargement was determined from a meter stick which was photographed beside the column.

Figures 13 and 14 of the appendix are photographs of the column enlarged to actual size. A close-up shot was made of the middle section of the column, making 10 to 15 cm. of the total 76 cm. available for studying the bubbles. It was calculated that a bubble would increase about 10 per cent in surface area from the bottom to the top of the column because of increase in temperature and decrease in pressure. For this reason, the middle section of the column was chosen for study to reduce this source of error.

All of the bubbles in the section having a sufficiently sharp image were measured, this number generally being between 300 and 400. This number comprised approximately 10 per cent of the total bubbles in the column and it was felt this was a sufficiently representative sample upon which to base a calculation of the average bubble diameter. It was recognized that the ultimate use of the average bubble diameter would be for the calculation of surface area and, therefore, an average was chosen which would give more weight to the d^2 term.

For this purpose the relation of Perrott and Kinney (2) was chosen. It is expressed by:

$$d_s = \frac{\Sigma nd^2}{\Sigma n} \qquad (4)$$

where: d_s = mean surface diameter, ft.

n = number of bubbles having an average diameter, d

and d = average diameter of each size group, ft.

Each bubble counted and measured was placed in a size group according to its diameter, each group representing a range of 0.25 mm. The average diameter of a group was taken as the arithmetic average of the size range of the group, e.g., a group of 40 bubbles having a diameter between 1.25 and 1.50 mm. would have an average group diameter of 1.38 mm. A typical size distribution of bubbles is given in Table 7 of the Appendix.

Two methods were used to determine the total number of bubbles in the column. A count was made of the number of bubbles in a 10 cm. section of the column and this figure was multiplied by the total height of water divided by 10. The second method was to note the volume of water in the column which was displaced by the air. This was done by measuring the change of level of the water in the column from zero air flow to the air flow rate of the experimental run. The average volume per bubble was calculated from a mean volume diameter (3) given by:

$$d_v = \frac{\sum nd^3}{\sum n} \qquad (5)$$

The same data were used to calculate d_v that were used to calculate d_s. Again, this relation was chosen because volume is proportional to d^3 and this expression gives more weight to the d^3 term.

The results of both methods compared rather well, the latter being 4 per cent higher. Both methods are subject

to errors due to coalescence of bubbles, deviation from spherical form, and distortion of the bubble images by the curved surface of the column.

The method of calculating the coefficient when the sintered glass plug was used differed from the previously discussed method in the following respects. When the ceramic plug was used, a run consisted of observations made at one instant of time, whereas for the sintered glass plug, data for one run were taken over periods of from 20 to 50 minutes in duration. It was necessary to use an integrated form of equation (1) for this case. The resulting relation may be written:

$$h = \frac{\int_0^T Gs_1 \, (tg - t_1) \; dT}{A \int_0^T \frac{(tw_b - t_1) - (tw_t - tg) \; dT}{\ln \frac{tw_b - t_1}{tw_t - tg}}} \qquad (6)$$

where: t_g = temperature of exit air, $^{\circ}F$

t_1 = temperature of entering air, $^{\circ}F$

tw_b = temperature of water at bottom of column, $^{\circ}F$

tw_1 = temperature of water at top of column, $^{\circ}F$

and T = time in minutes

The water was not circulated and it was found in this case that it was at a uniform temperature over the entire

length of the column. Equation (6) then simplifies to

$$h = \frac{Gs_1 \int_0^T (tg-t_1)\, dT}{A \int_0^T \frac{tg-t_1}{\ln \frac{tw-t_1}{tw-tg}}\, dT} \qquad (7)$$

where: tw = average water temperature, ^{o}F

Equation (7) involved two graphical integrations of $(tg-t_1)$ versus T and $\frac{tg-t_1}{\ln \frac{tw-t_1}{tw-tg}}$ versus T which are shown in Figures 11 and 12 of the Appendix. There was very little variation in the absolute humidity of the entering air and, therefore, its heat capacity, s_1, does not appear under the integral sign in equation (7). Obviously, the area is also independent of time and appears as a constant.

The bubble areas were determined in the same manner as previously used with the ceramic plug.

Table 1. Calculated Heat Transfer Coefficients for Individual Runs with Ceramic Plug.

Run No.	Flow Rate Air, Lbs./hr.	Flow Rate Water, Lbs./hr.	Bubble Diam., Ft.	Total Surface Area, Ft^2.	h, BTU $hr./Ft^2./^oF$
1	0.222	0.208	0.0108	1.22	0.00947
2	0.222	0.208	0.0108	1.22	0.0137
3	0.222	0.208	0.0108	1.22	0.0168
14	0.222	0.208	0.0108	1.22	0.0226
20	0.222	0.208	0.0108	1.22	0.0161
23	0.222	0.208	0.0108	1.22	0.0262
29	0.222	0.208	0.0108	1.22	0.0181
33	0.222	0.208	0.0108	1.22	0.0139
34	0.222	0.208	0.0108	1.22	0.0242
5	0.151	0.208	0.00839	0.776	0.0167
6	0.151	0.208	0.00839	0.776	0.0161
7	0.151	0.208	0.00839	0.776	0.0150
8	0.151	0.208	0.00839	0.776	0.0156
15	0.151	0.208	0.00839	0.776	0.00666
21	0.151	0.208	0.00839	0.776	0.0184
24	0.151	0.208	0.00839	0.776	0.0101
30	0.151	0.208	0.00839	0.776	0.0170
9	0.0746	0.208	0.00798	0.492	0.00940
10	0.0746	0.208	0.00798	0.492	0.00760
11	0.0746	0.208	0.00798	0.492	0.00704
12	0.0746	0.208	0.00798	0.492	0.00570
13	0.0746	0.208	0.00798	0.492	0.00557
16	0.0746	0.208	0.00798	0.492	0.00651
22	0.0746	0.208	0.00798	0.492	0.0120
25	0.0746	0.208	0.00798	0.492	0.00604
31	0.0746	0.208	0.00798	0.492	0.00838
18	0.222	0.483	0.00938	1.18	0.0152
27	0.222	0.483	0.00938	1.18	0.0190
37	0.222	0.483	0.00938	1.18	0.0281
41	0.222	0.483	0.00938	1.18	0.0363
17	0.151	0.483	0.00856	0.828	0.0106
26	0.151	0.483	0.00856	0.828	0.0121
36	0.151	0.483	0.00856	0.828	0.0186
40	0.151	0.483	0.00856	0.828	0.0193
19	0.0746	0.483	0.00698	0.546	0.00868
28	0.0746	0.483	0.00698	0.546	0.00730
32	0.0746	0.483	0.00698	0.546	0.00476
42	0.151	0.0	0.00839	0.776	0.00952
43	0.151	0.0	0.00839	0.776	0.0172

Table 2. Calculated Heat Transfer Coefficients for Individual Runs with Sintered Glass Plug.

Run No.	Flow Rate Air Lbs./hr.	Bubble Diam., Ft.	Area Ft^2.	h, $\frac{BTU}{hr./Ft^2./^\circ F}$
2	0.222	0.0117	1.13	0.0201
4	0.222	0.0117	1.13	0.0153
1	0.151	0.0103	0.546	0.0201
6	0.151	0.0103	0.483	0.00978
5	0.151	0.0103	0.540	0.0126
3	0.0746	0.00294	0.355	0.00308

Table 3. Summary of Results

Flow Rate Air, Lbs./hr.	Flow Rate Water, Lbs./hr.	Bubble Diam., d_s, cm.	Total Area, A, Ft^2	Ave. h $\frac{BTU}{hr./Ft^2/^oF}$	No. of Runs Averaged	Average Deviation
0.0746	0.483	0.213	0.546	0.00691	3	$\pm$ 0.00261
0.0746	0.208	0.244	0.492	0.00758	9	$\pm$ 0.00157
0.0746	0.0	0.0895	0.355	0.00308	1	
0.151	0.483	0.261	0.828	0.0152	5	$\pm$ 0.00382
0.151	0.208	0.256	0.776	0.0137	7	$\pm$ 0.00318
0.151	0.0	0.256	0.776	0.0134	2	
0.151	0.0	0.316	0.546	0.0142	3	$\pm$ 0.00385
0.222	0.483	0.286	1.186	0.0247	4	$\pm$ 0.00754
0.222	0.208	0.3275	1.22	0.0179	9	$\pm$ 0.00454
0.222	0.0	0.357	1.13	0.0177	2	

CHAPTER IV

DISCUSSION OF RESULTS

Heat transfer coefficients for each run with the ceramic plug in the column are presented in Table 1. Table 2 is composed of coefficients calculated for individual runs with the sintered glass plug, and Table 3 is a summary of average coefficients for each flow rate of air and water.

It can be seen from these tables that the coefficients cover the range from 0.00308 to 0.0363, depending upon flow rates and bubble size. It will also be noted from the tables that, for both methods of calculating the coefficients, the numerical values were of the same order of magnitude for comparable air flow rates, and that any difference in the two might be attributed to the different water flow rates which were used with the ceramic plug.

It might seem from first inspection that the calculated coefficients of heat transfer were rather low as compared to coefficients obtained by other methods of heating air, as in the case of air flowing over tubes in a conventional heat exchanger. It must be remembered, however, that this is an entirely different case, and, as such, cannot be compared with such conventional cases as heat exchangers.

An analogy can be drawn, however, with the case of hot gases passing through a packed bed of spherical particles,

a study of which was made by Gamson, Thodos and Hougen (4). They calculated heat transfer coefficients based on heat transfer through an air film surrounding a solid spherical particle. Their mass flow rates of air were considerably higher than those encountered in this investigation, but an equation was given for extrapolation of their data to Reynolds numbers less than 40. This equation is:

$$j_h = 18.1 \frac{D_p G}{\mu} - 1 \qquad (8)$$

where: j_h = heat transfer factor

$\frac{D_p G}{\mu}$ = modified Reynolds number

D_p = particle diameter, ft.

μ = absolute viscosity of gas film, $\frac{\text{lb.}}{\text{hr./ft.}}$

j_h is given by equation (9):

$$j_h = \frac{h}{c_p G} \frac{c_p \mu}{k}^{2/3} \qquad (9)$$

where: k = thermal conductivity of air $\frac{\text{BTU}}{\text{hr./ft}^2/^{\circ}\text{F/ft.}}$

and c_p = heat capacity of air, $\frac{\text{BTU}}{\text{lb./}^{\circ}\text{F}}$.

By taking D_p equal to a bubble diameter with G and μ taken from the experimental data corresponding to this bubble diameter, a j_h could be calculated by equation (8). This was done for a bubble diameter of 0.0117 ft. and a corresponding Reynolds number of 2.71. The result of this calculation indicated a coefficient of 19.7 $\frac{\text{BTU}}{\text{hr./ft}^2/^{\circ}\text{F}}$. These figures

can possibly be reconciled by the difference of the areas upon which the two calculations are based.

The area used by Gamson, et al., was based on the surface area of the solid particle having a diameter D_p and a surrounding air film of unknown thickness. Assuming a very thin air film, this is approximately the true area through which heat is being transferred. However, in the case of the bubble, the surface area of the bubble is not the true area if the entire mass of air can be considered as stagnant. In this case, the thickness of the film becomes equal to the radius of the bubble, and the area for heat transfer becomes the geometric mean of the outside surface area and the area of a sphere having a radius r_1, r_1 being a very small increment of the total radius. The geometric mean area (5) would be given in such a case by:

$$A_m = \sqrt{(4\pi r_1)^2 \, (\pi D_p)^2} \quad . \tag{10}$$

If r_1 is taken as 1×10^{-5} ft. and D_p as 0.0117 ft., then $A_m = 3.69 \times 10^{-7}$ ft.^{2} as compared to a surface area A of 4.33×10^{-4} ft.^{2} Multiplying the experimental coefficient of 0.0177 by the ratio $\frac{4.33 \times 10^{-4}}{3.69 \times 10^{-7}}$, it becomes 20.8 $\frac{\text{BTU}}{\text{hr./ft.}^2/^{\circ}\text{F}}$, as compared with Gamson's value of 19.7 $\frac{\text{BTU}}{\text{hr./ft.}^2/^{\circ}\text{F}}$. This does not mean to imply that the value of 20.8 $\frac{\text{BTU}}{\text{hr./ft.}^2/^{\circ}\text{F}}$ is an actual value of the coefficient, since the choice of r_1 is an arbitrary one. It is intended merely to illustrate the effect of choosing a different basis for calculating the area available

for heat transfer by a bubble. It also serves to show that the air inside the bubble is possibly stagnant and acts as a film having a thickness substantially equal to the radius of the bubble. Such a film would offer a high resistance to heat flow. This is only a hypothesis, however, which cannot be proven or disproven at the present time.

An effort was made to apply Fourier's law of heat conduction by considering the bubble as a solid sphere, but this proved to be of little value in predicting what the temperature of the bubble would be at any time. The rigorous mathematical approach was precluded, because the assumption that a bubble could be treated as a solid was not a valid one. The mechanism of heat transfer in a gas is entirely different from that of a solid. Energy transfer in a gas takes place by momentum transfer between molecules, whereas heat is transferred in non-conducting solids by longitudinal oscillations and in metals by motion of electrons. It must also be kept in mind that for the air molecule to receive heat from the water, it must make contact with the water at the gas-water interface. A large part of this interfacial area will be obstructed by water vapor molecules diffusing into the bubble due to the partial pressure driving force. However, one can only surmise what actually takes place, and as Jakob states, "From a quantitative viewpoint, however, it should not be forgotten that it is not known yet whether heat transfer on a liquid surface (without phase change) follows the same law as heat transfer on a solid surface." (6)

No attempt was made to measure experimentally bubble velocity, but Garber and Peebles (7) have correlated bubble radius with terminal velocity. This correlation is shown in Figure 2. These bubble velocities were obtained by observing single bubbles rising in a column and, therefore, do not apply strictly in this case. Some idea can be gained, however, of the magnitude of the velocities from their correlation. When the coefficients are plotted against bubble radius on log-log coordinates, there is a sharp increase in the slope of the curve at a bubble radius of 0.004 ft. This is shown in Figure 3. A sharp inflection point also occurs at a bubble radius of 0.0035 on a curve of bubble radius against terminal velocity. This would indicate, then, that bubble radius and terminal velocity have a pronounced effect upon the heat transfer coefficient, but these variables were not studied over a wide enough range to formulate any definite statement or equation as to their exact relationship.

The heat transfer coefficient was also plotted against Reynolds number and mass velocity of air, both curves yielding almost straight line relationships with h increasing with increasing Reynolds number and increasing mass flow, as shown in Figures 4 and 5.

It would be desirable to be able to state more quantitatively which variables affect the heat transfer coefficient and how they affect it, but the limited data prohibit doing

this. There were no previous data to aid in correlation, and it is only possible to point the way for more extensive study.

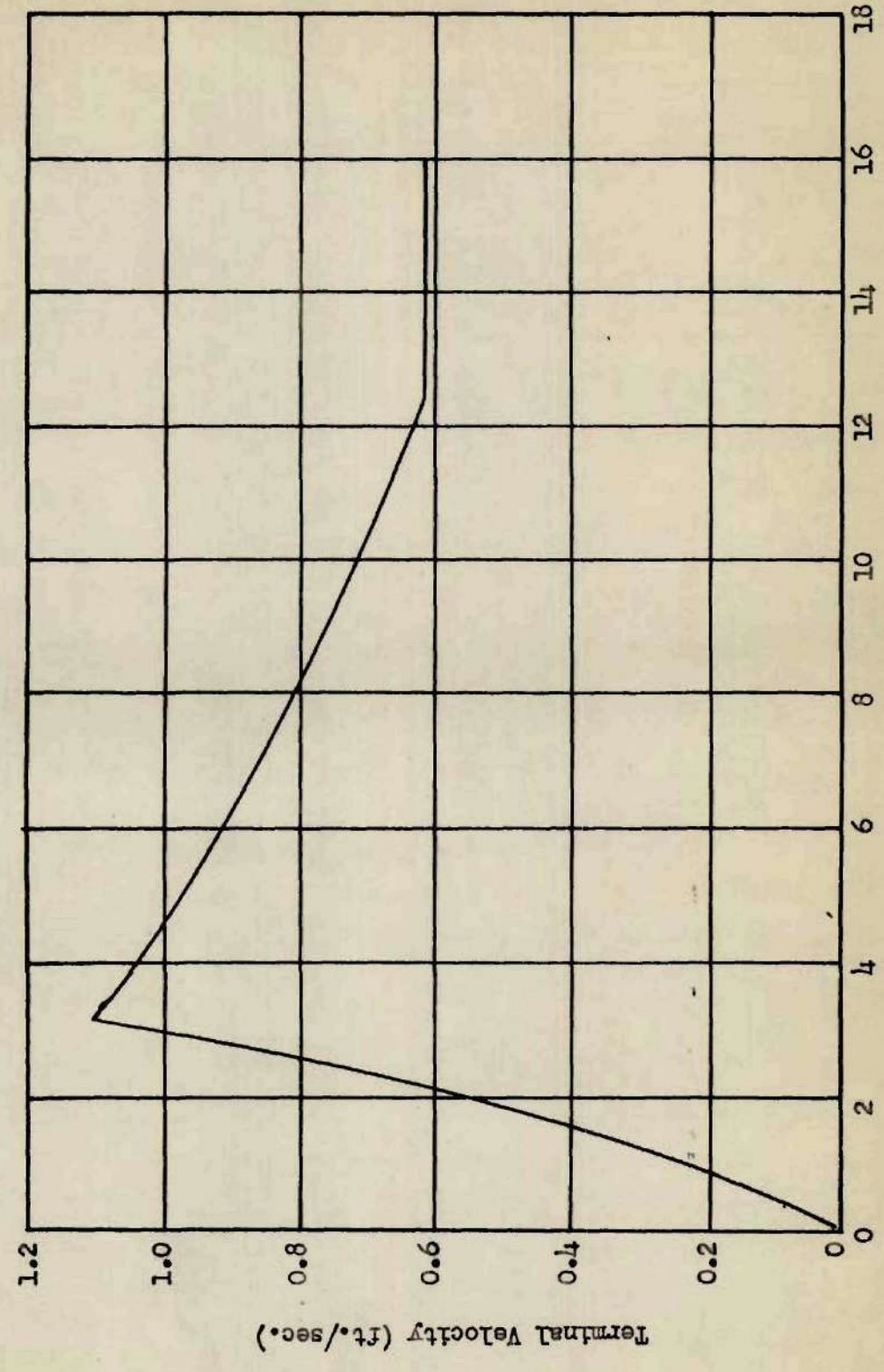

Figure 2. Garber and Peebles Correlation of Bubble Radius with Terminal Velocity

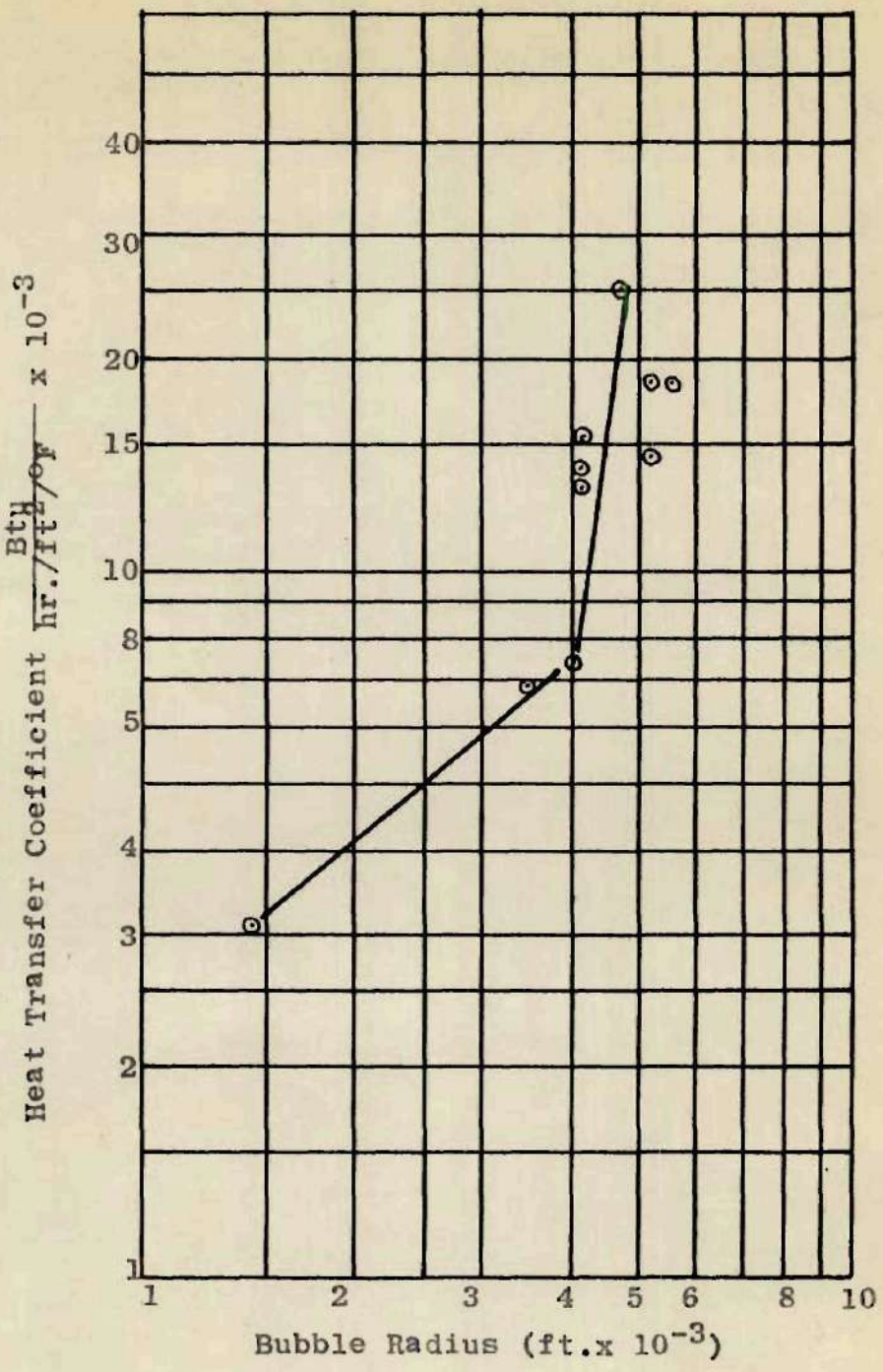

Figure 3. Experimental Heat Transfer Coefficient as Function of Bubble Radius.

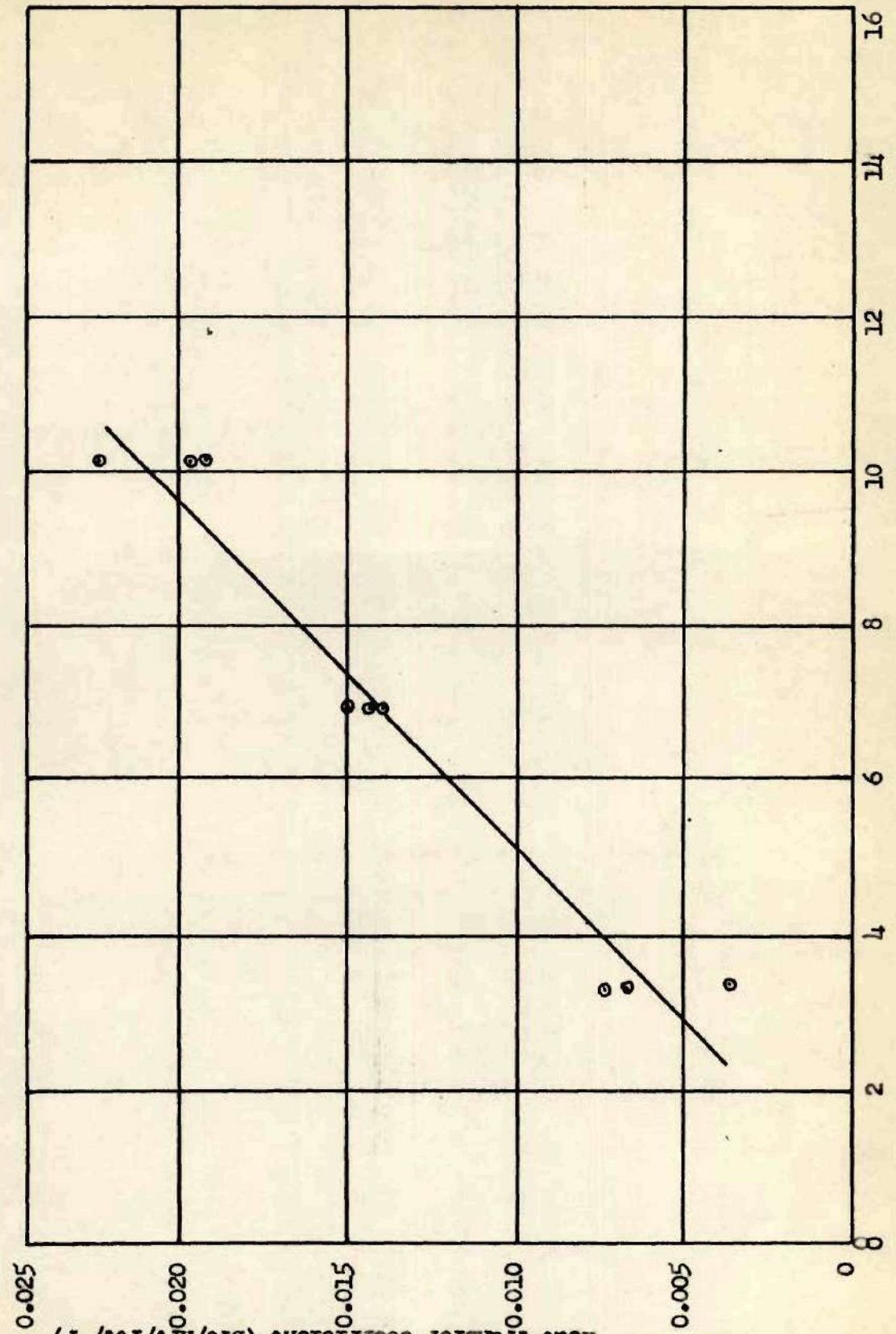

Figure 4. Relation of Experimental Heat Transfer Coefficients to Mass Flow Rate of Air

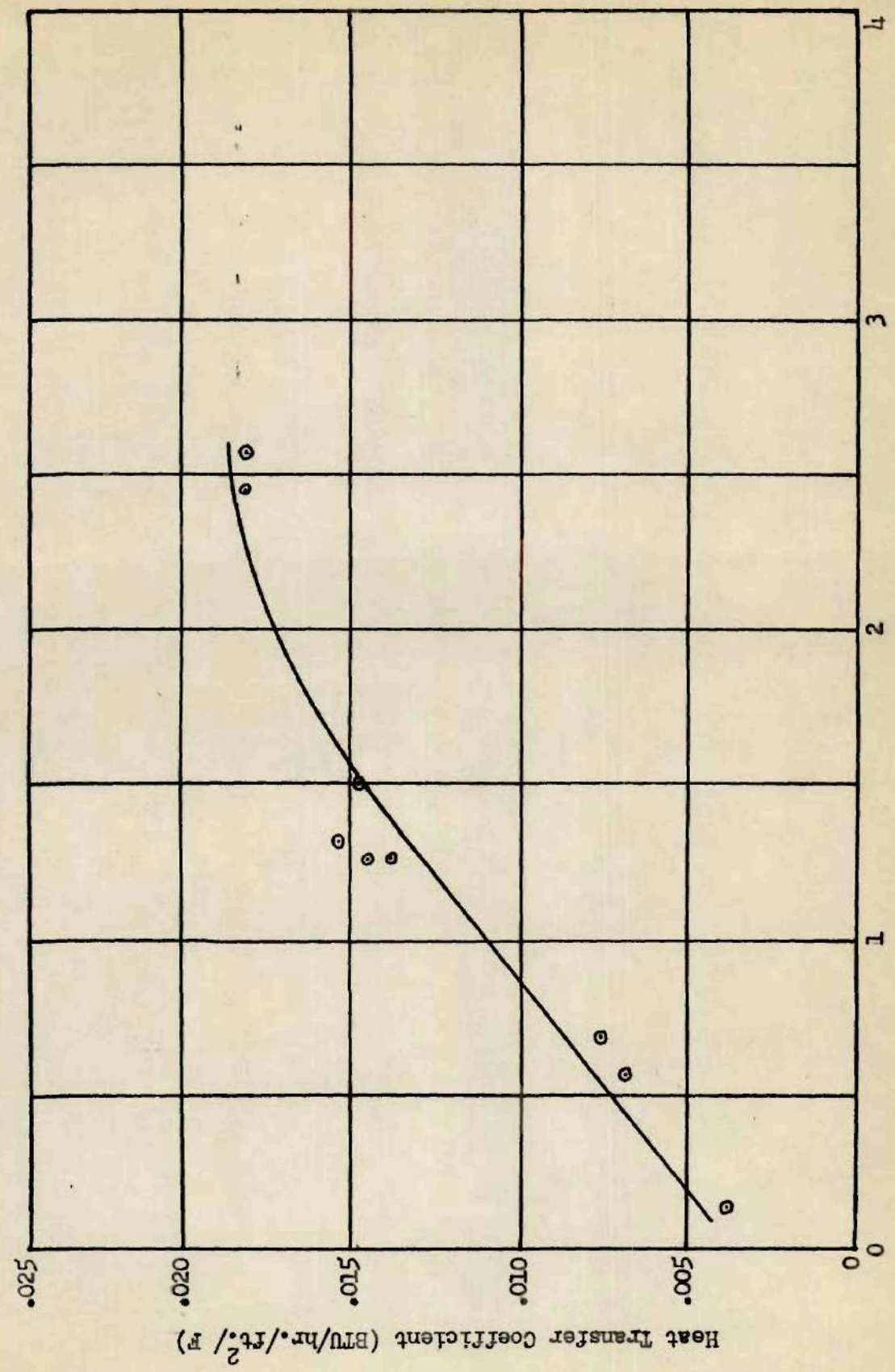

Figure 5. Heat Transfer Coefficient as a Function of Reynolds Number

CHAPTER V

CONCLUSIONS

It can be concluded from the results of this investigation that air bubbles offer very high resistance to heat transfer as compared to other methods of transferring heat between gases and liquids. It was also shown that the heat transfer coefficient increased with increasing mass flow rate, increasing bubble radius, and increasing Reynolds number. Bubble radius and Reynolds number are functions of mass flow rate, so it would seem that air flow rate was the controlling factor in this case. This conclusion presupposes no change in the size or type of porous plate employed to produce the bubbles; otherwise, bubble radius becomes a function of the plate pore size as well as flow rate.

It might be inferred from consideration of other heat transfer cases that other physical properties of the gas and liquid such as viscosity, density, and surface tension are also factors which must be considered in any attempt to predict heat transfer coefficients in other systems. These variables were not studied in this initial investigation, however, so their effect on the coefficients which were calculated is not readily apparent.

CHAPTER VI

RECOMMENDATIONS

It is recommended that any subsequent investigation along this line be carried out on a larger scale, employing larger flow rates of air to reduce the effect of errors made in flow rate and temperature measurements.

It is further recommended that other gases and liquids be used over wide ranges of flow rates and bubble sizes to facilitate correlation of the data.

APPENDIX

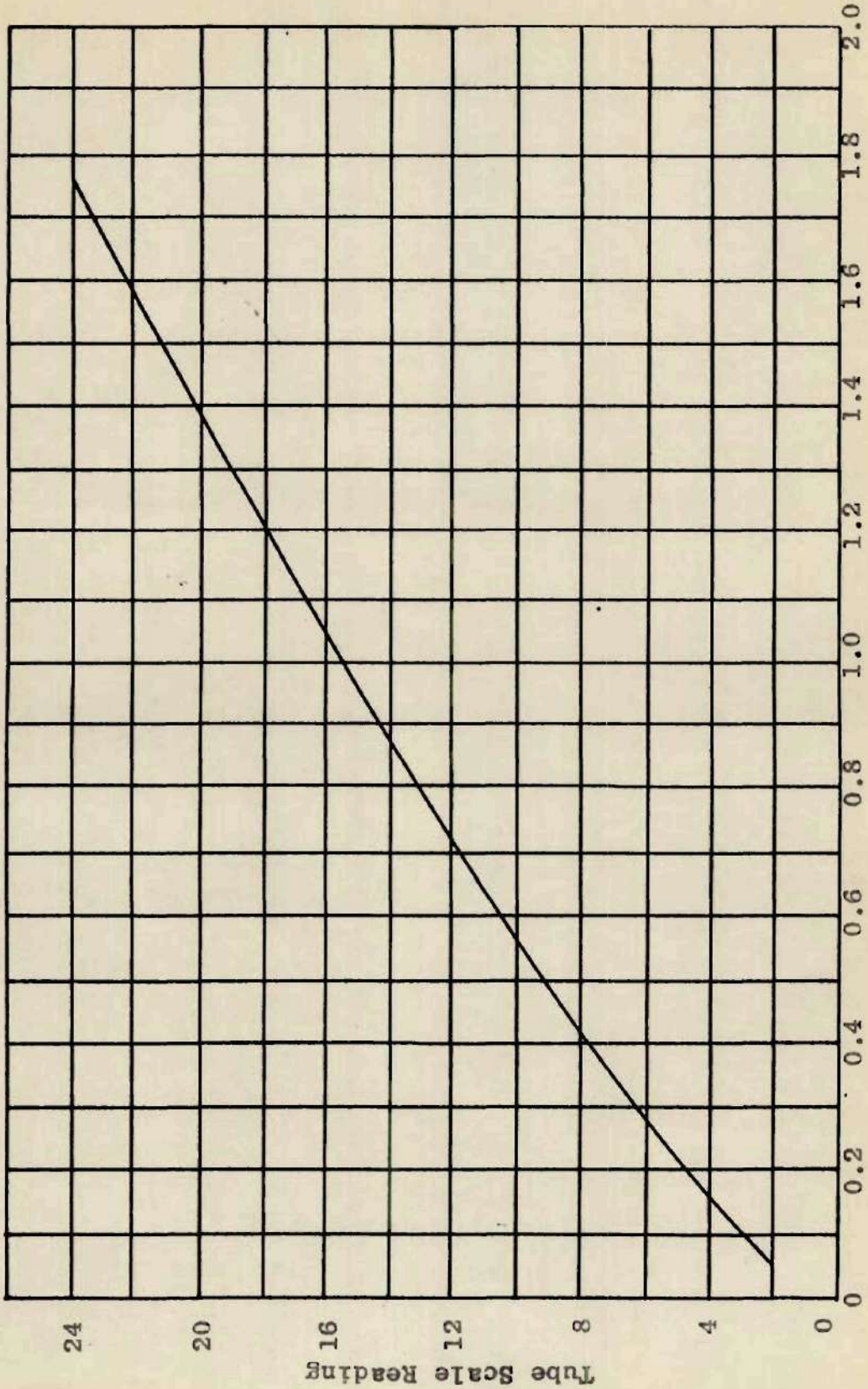

Figure 6. Rotameter Calibration Curve for Water.

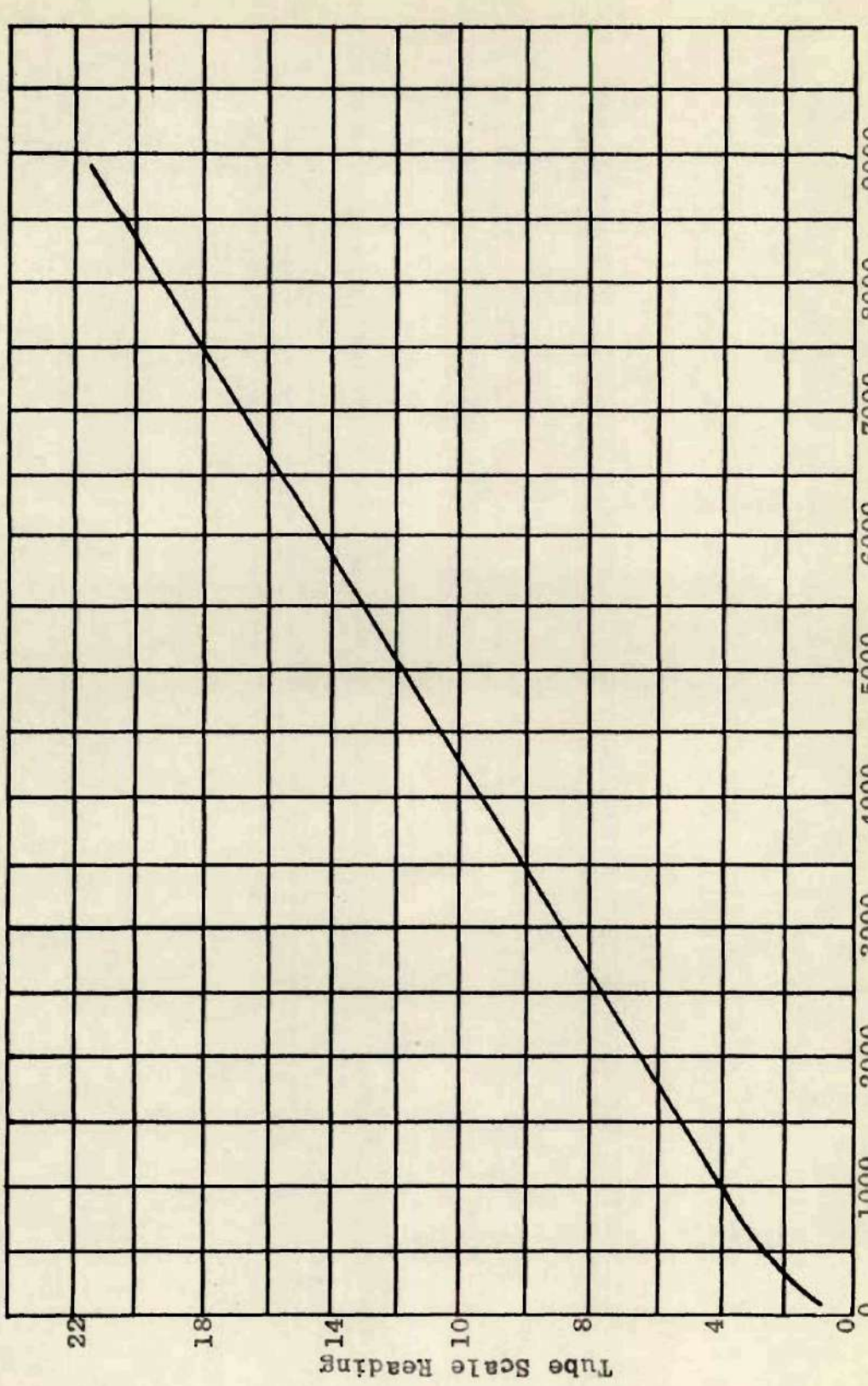

Figure 7. Rotameter Calibration Curve for Air

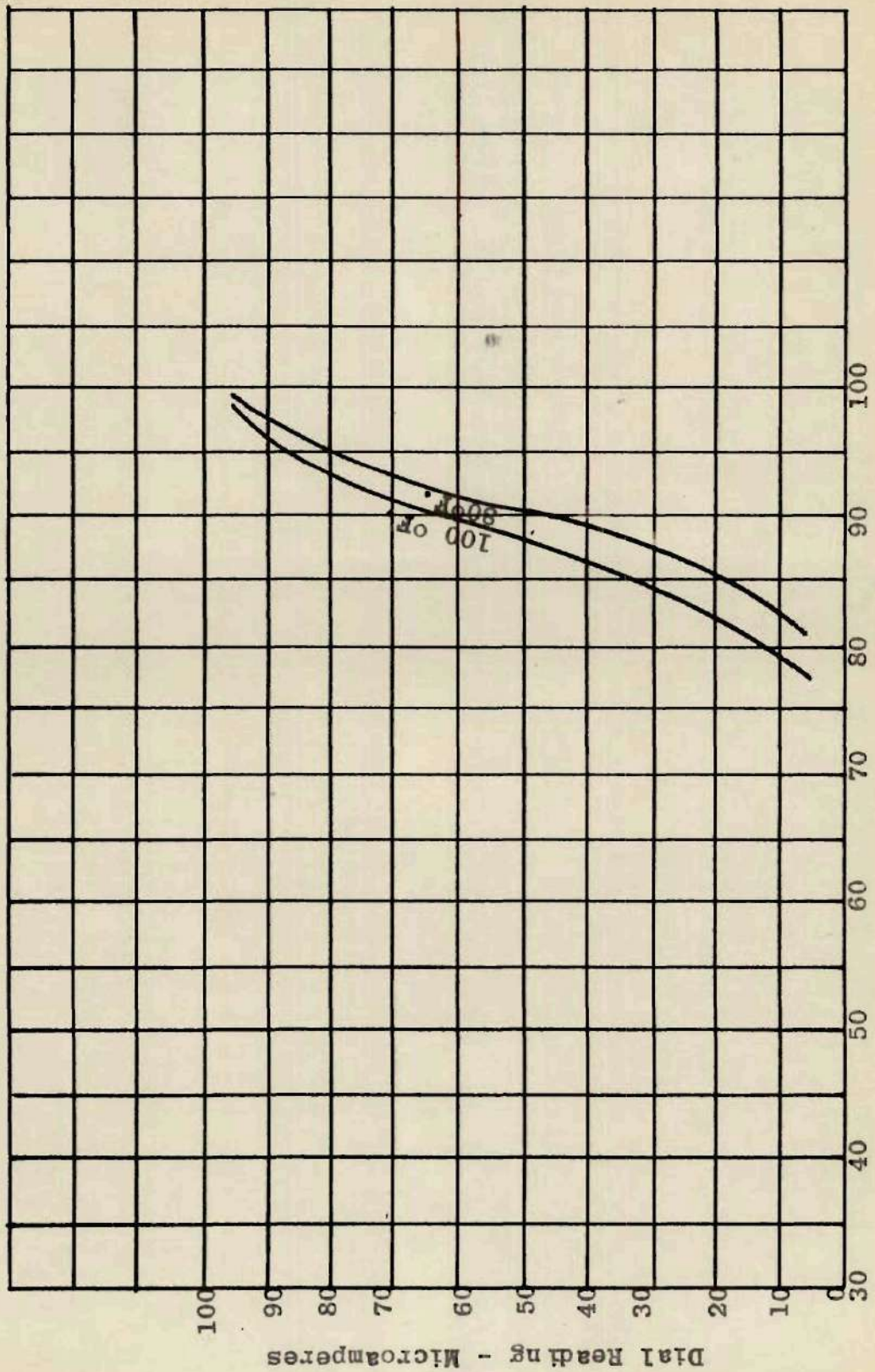

Figure 8. Electric Hygrometer Calibration Curve for Exit Air.

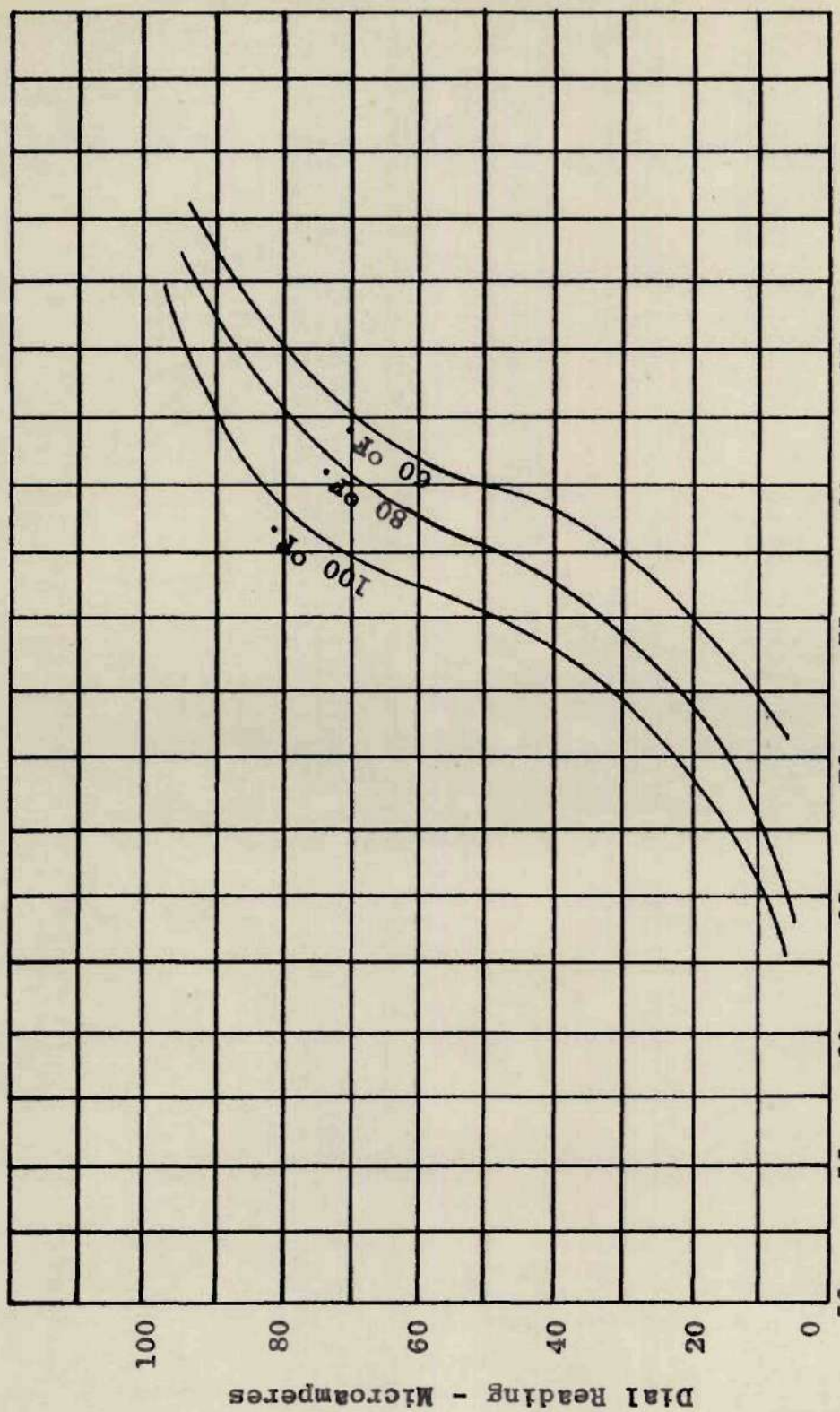

Figure 9. Electric Hygrometer Calibration Curve for Entering Air.

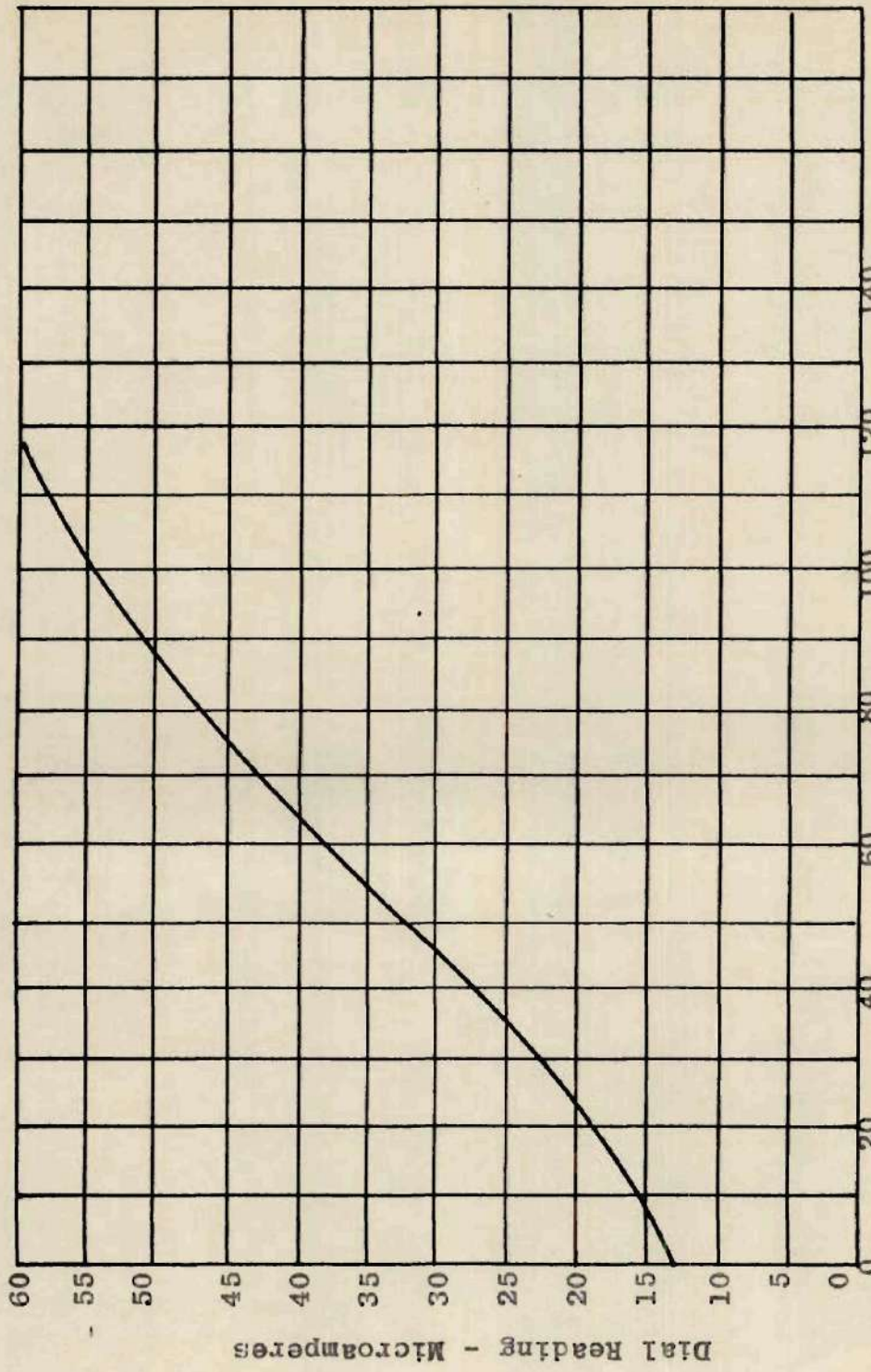

Figure 10. Electric Hygrometer Temperature Calibration Curve

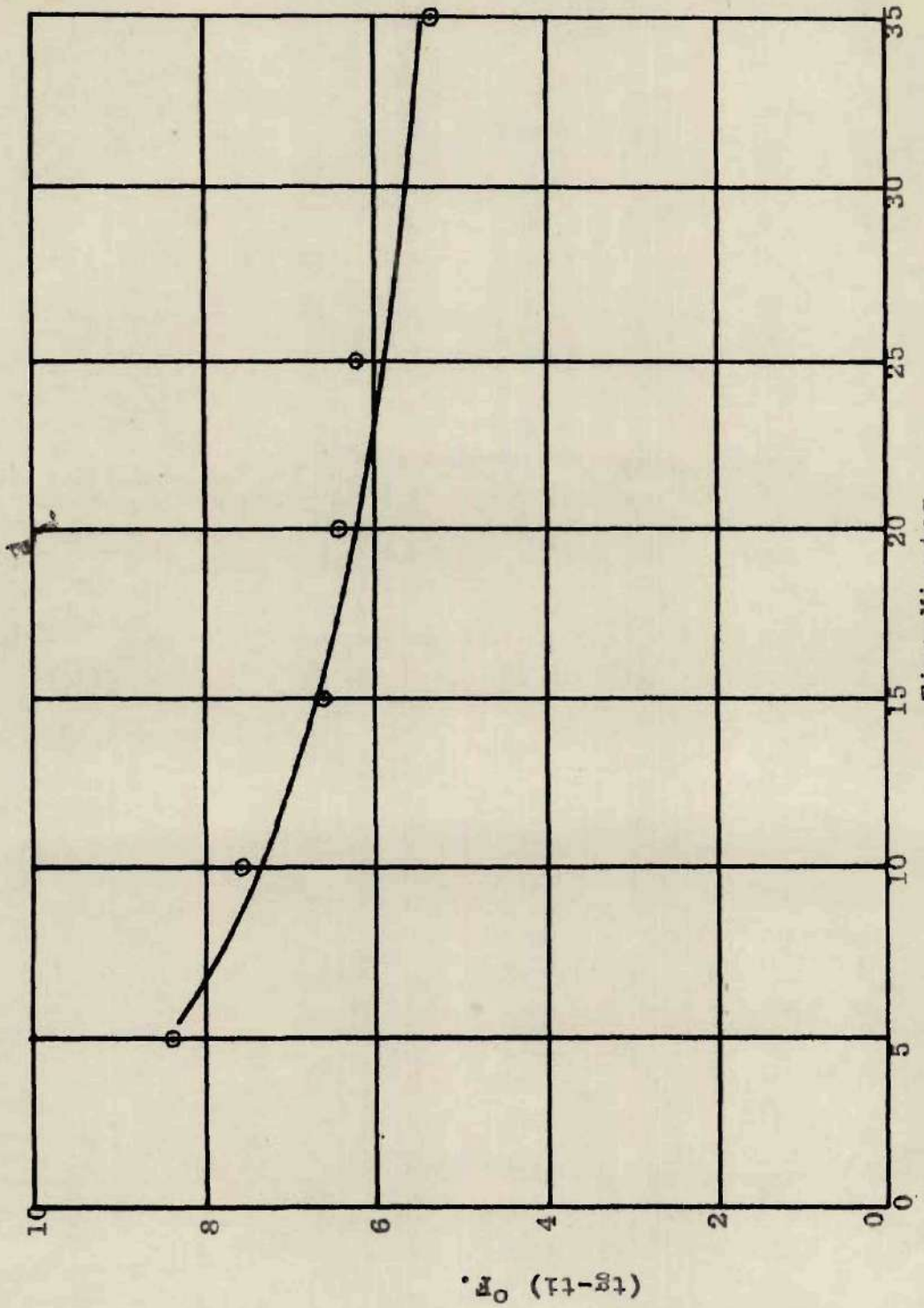

Figure 11. Typical Curve of (tg-ti) Against Time With Sintered Glass Plug -- Run No. 2.

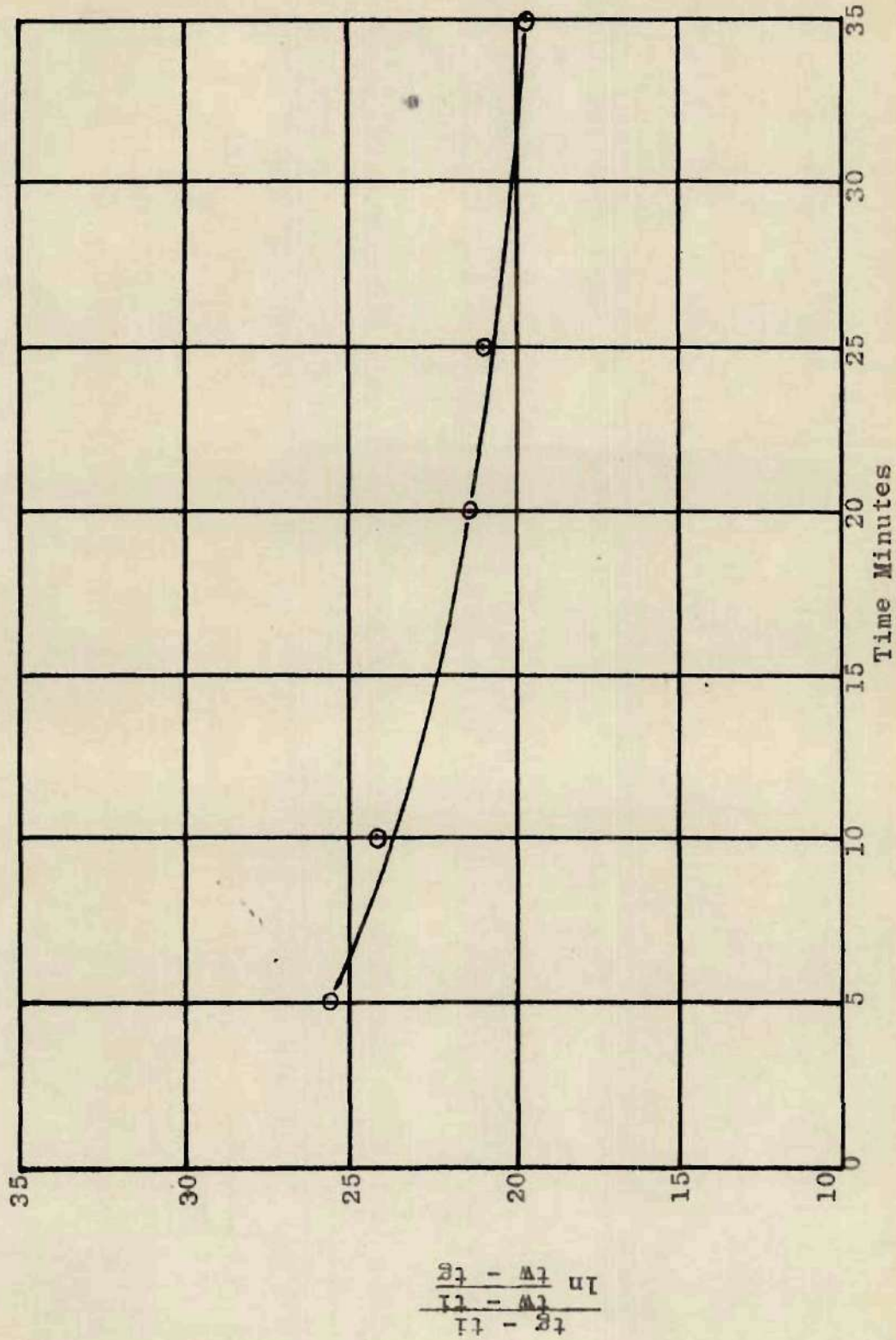

Figure 12. Typical Curve of $\frac{tg - ti}{\ln \frac{tw - ti}{tw - tg}}$ Against Time With Sintered Glass Plug -- Run No. 2.

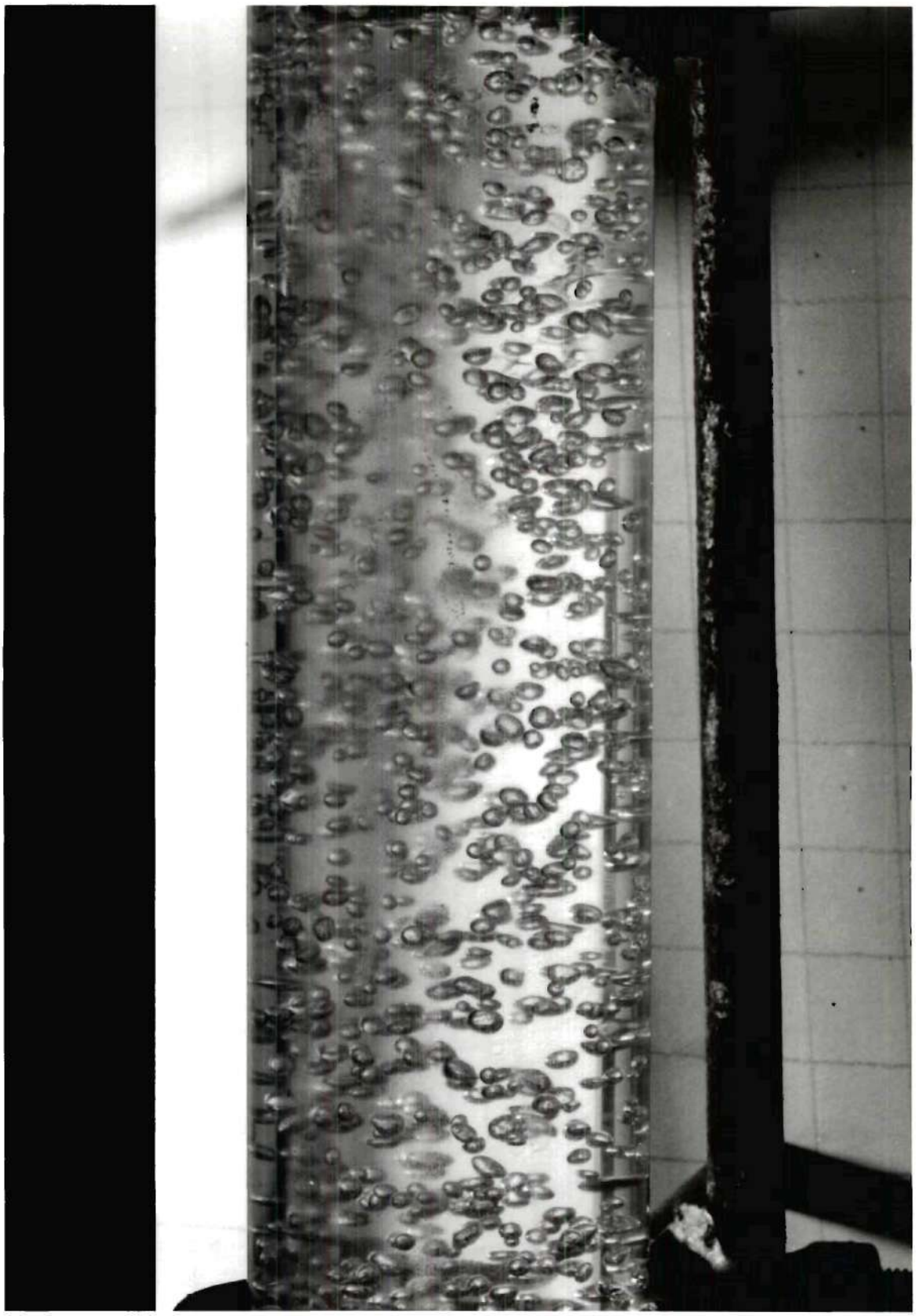

Figure 13. High Speed Photograph of Column with Bubbles Produced by Sintered Glass Plug.

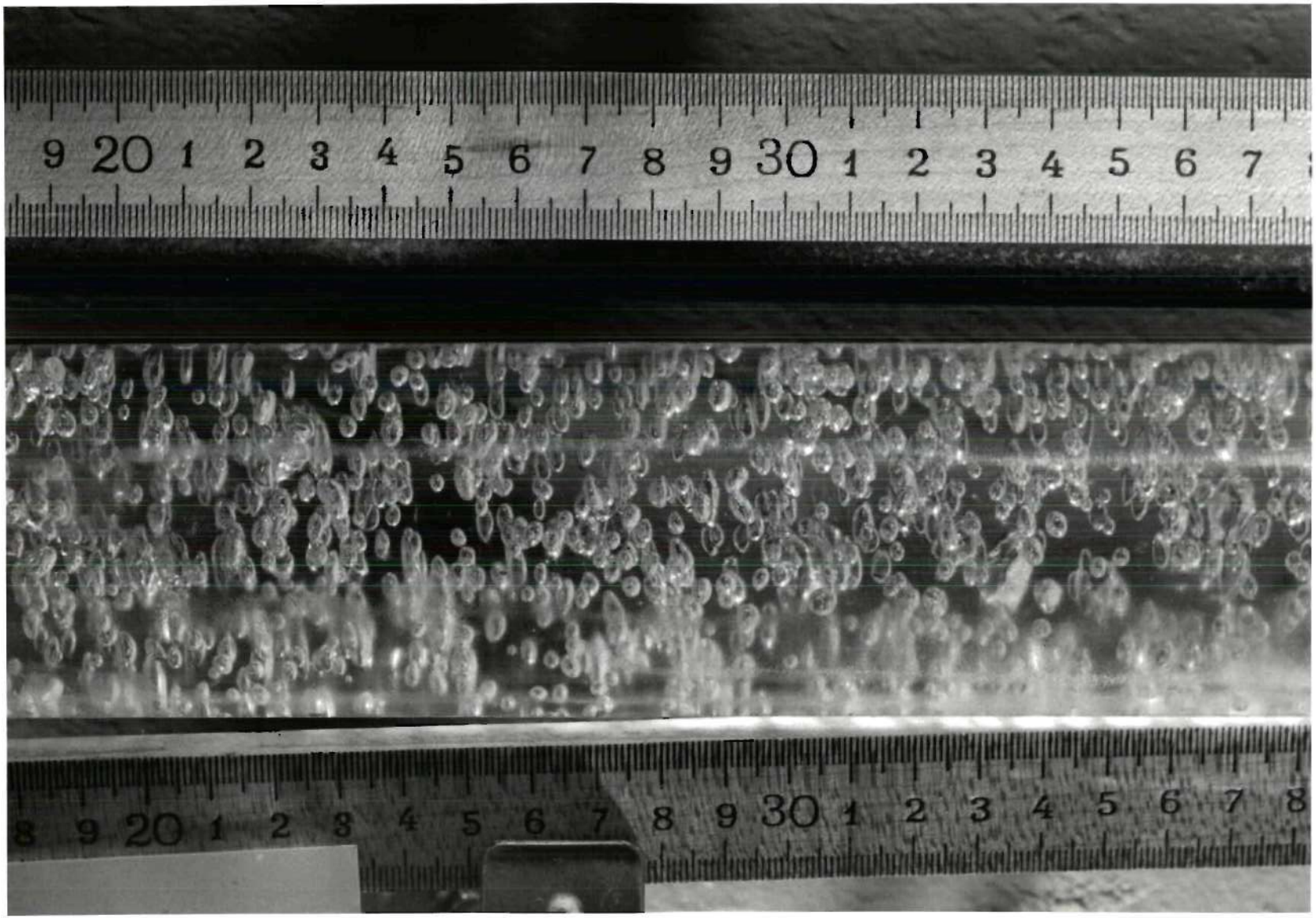

Figure 14. High Speed Photograph of Column with Bubbles Produced by Ceramic Plug.

Table 4. Experimental Data (Ceramic Plug)

Run No.	Air In Temp. °C	Air Out Temp. °C	Water In Temp. °C	Water Out Temp. °C
1	25.8	29.2	45.8	41.4
2	25.8	30.6	45.9	42.2
3	25.9	31.7	45.9	42.8
4	25.8	32.0	46.0	43.1
5	25.8	31.4	45.6	43.4
6	25.8	31.3	46.0	43.6
7	25.9	31.0	46.0	43.8
8	25.8	31.2	46.0	44.0
9	25.9	30.1	45.8	44.1
10	25.9	29.4	46.0	44.3
11	25.9	29.2	46.0	44.3
12	26.0	28.7	45.9	44.4
13	26.0	28.6	46.0	44.4
14	28.6	35.2	46.8	43.8
15	26.4	28.9	45.4	44.3
16	26.4	29.3	45.3	44.0
17	26.4	30.2	45.2	44.4
18	27.7	32.5	45.2	44.5
19	27.6	21.6	45.3	44.7
20	27.4	32.8	45.8	44.2
21	27.2	32.9	46.0	44.4
22	27.4	31.6	46.0	44.4
23	28.2	35.8	46.4	44.3
24	26.4	29.9	45.2	44.1
25	26.4	29.1	45.2	44.0
26	26.4	30.8	45.2	44.6
27	27.6	33.4	45.4	44.5
28	27.6	31.0	45.4	44.7
29	27.4	33.3	46.0	44.3
30	27.4	32.8	46.0	44.4
31	27.4	31.0	45.9	44.4
32	27.4	29.8	45.5	44.9
33	25.2	30.2	44.8	43.0
34	25.9	33.3	45.2	43.6
35				
36	25.8	32.3	45.3	44.2
37	25.9	34.6	45.3	44.4
38				
39				
40	25.8	32.5	45.2	44.3
41	25.9	35.7	45.4	44.5

Table 4. Experimental Data (Ceramic Plug)
(Continued)

Run No.	Flow Rate Air lbs./hr.	Flow Rate H_2O lbs./hr.	Air In Humidity lbs. H_2O / lb. Dry Air	Air Out Humidity lbs. H_2O / lb. Dry Air
1	0.222	0.208	0.0176	0.0260
2	0.222	0.208	0.0176	0.0280
3	0.222	0.208	0.0182	0.0300
4	0.222	0.208	0.0179	0.0305
5	0.151	0.208	0.0179	0.0295
6	0.151	0.208	0.0179	0.0295
7	0.151	0.208	0.0182	0.0287
8	0.151	0.208	0.0179	0.0290
9	0.0746	0.208	0.0184	0.0272
10	0.0746	0.208	0.0184	0.0263
11	0.0746	0.208	0.0184	0.0260
12	0.0746	0.208	0.0184	0.0252
13	0.0746	0.208	0.0183	0.0250
14	0.222	0.208	0.0197	0.0370
15	0.151	0.208	0.0185	0.0255
16	0.0746	0.208	0.0185	0.0260
17	0.151	0.483	0.0185	0.0275
18	0.222	0.483	0.0206	0.0313
19	0.0746	0.483	0.0208	0.030
20	0.222	0.208	0.0206	0.0320
21	0.151	0.208	0.0197	0.0320
22	0.0746	0.208	0.0203	0.0300
23	0.222	0.208	0.0190	0.0380
24	0.151	0.208	0.0185	0.0270
25	0.0746	0.208	0.0185	0.0260
26	0.151	0.483	0.0184	0.0285
27	0.222	0.483	0.0204	0.0330
28	0.0746	0.483	0.0208	0.0290
29	0.222	0.208	0.0201	0.0330
30	0.151	0.208	0.020	0.0320
31	0.0746	0.208	0.0205	0.0290
32	0.0746	0.483	0.0208	0.0270
33	0.222	0.208	0.0184	0.0275
34	0.222	0.208	0.0184	0.0275
35	0.151			
36	0.151	0.483	0.0180	0.0285
37	0.222	0.483	0.0140	0.0260
38				
39				
40	0.151	0.483	0.0140	0.0275
41	0.222	0.483	0.0140	0.0340

Table 5. Experimental Data
Zero Water Flow Rate (Ceramic Plug)

Run 42

Time minutes	0	5	10	15	20
Entering air temp. °C	24.9	24.9	24.9	24.9	24.7
Exit air temp. °C	26.9	27.3	27.6	27.3	27.2
Water temp. °C	39.7	40.8	39.8	39.1	38.2
Entering air % Rel. Humid.	87.5	87.5	87.5	87.5	87.5
Exit air % Rel. Humid.	100	100	100	100	100

Air Flow Rate = 0.151 $\frac{\text{lbs.}}{\text{hr.}}$

Height of Water in Column = 30.2 inches

Atmospheric Pressure = 28.95 inches Hg.

Air Pressure Entering Column = 32.6 inches Hg. absolute

Run 43

Time minutes	0	5	10	15	20	25	30
Entering air temp. °C	24.6	24.8	24.8	24.8	24.8	24.8	24.8
Exit air temp. °C	28.0	29.1	29.5	29.6	29.5	29.4	28.8
Water temp. °C	44.0	42.8	42.0	41.0	40.4	39.8	39.0
Entering air % Rel. Humid.	83	83	83	83	83	83	83
Exit air % Rel. Humid.	100	100	100	100	100	100	100

Air Flow Rate = 0.151 $\frac{\text{lbs.}}{\text{hr.}}$

Height of Water in Column = 30.2 inches

Atmospheric Pressure = 29.92 inches Hg.

Air Pressure Entering Column = 33.5 inches Hg. absolute

Table 6. Experimental Data (Sintered Glass Plug)

Run 1

Time minutes	0	5	10	15	20	25	40
Water Temp. °C							
Bottom	42.9	42.3	41.7	42.3	40.7	40.4	38.9
Middle	42.8	42.0	41.7	42.0	40.7	40.0	38.8
Top	42.8	42.2	41.8	42.2	40.7	40.2	39.0
Exit air temp. °C	30.5	30.3	30.4	30.3	30.2	30.1	29.6
Entering air temp. °F	80.5	78.3	79.0	80.0	80.0	80.0	80.0
Entering air % Rel.Humid.	90.5	91	90.5	91.5	91.5	91.5	91.5
Exit air % Rel. Humid.	100	100	100	100	100	100	100

Height of water in column = 29.25 inches

Flow Rate of Air = 0.151 $\frac{\text{lbs.}}{\text{hr.}}$

Atmospheric Pressure = 29.92 inches Hg.

Room Temperature = 79°F

Run 2

Time minutes	0	5	10	15	20	25	30	40
Water Temp. °C								
Bottom	43.6	42.9	42.2	41.8	41.2	40.7	40.2	39.2
Middle	43.7	43.0	42.4	42.0	41.3	40.9	40.2	39.2
Top	43.8	42.9	42.4	41.8	41.2	40.7	40.2	39.2
Exit air temp. °C	32.2	32.3	32.1	32.5	32.2	32.0	32.4	32.1
Entering air temp. °F	83.7	83.2	83.7	83.7	81.7	81.2	81.2	81.0
Entering air % Rel. Humid.	90	90	90	90	90	90	90	90
Exit air % Rel. Humid.	100	100	100	100	100	100	100	100

Height of water in column = 28 inches

Flow Rate of Air = 0.222 $\frac{\text{lbs.}}{\text{hr.}}$

Atmospheric Pressure = 29.92 inches Hg.

Room Temperature = 81°F

Table 6. Experimental Data (Sintered Glass Plug) (Continued)

Run 3

Time minutes	0	5	10	15	20	25
Water Temp. °C						
Bottom	44.1	43.2	42.7	42.2	41.7	41.4
Middle	44.1	43.2	42.8	42.2	41.9	41.5
Top	44.1	43.2	42.7	42.3	41.8	41.4
Exit air temp. °C	28.4	28.4	28.4	28.4	28.3	28.3
Entering air temp. °F	81.2	82.4	81.7	81.7	81.2	81.2
Entering air % Rel. Humid.	92	92	92	92	92	92
Exit air % Rel. Humid.	100	100	100	100	100	100

Height of water in column = 30 inches

Flow Rate of Air = 0.0746 $\frac{\text{lbs.}}{\text{hr.}}$

Run 4

Time minutes	0	5	10	15	20	25	30	40	50
Water Temp. °C									
Bottom	41.2	40.6	40.1	39.7	39.2	38.8	38.4	37.6	37.0
Middle	41.1	40.6	40.1	39.8	39.2	39.0	38.5	37.8	37.0
Top	41.2	40.6	40.1	39.7	39.2	38.9	38.4	37.7	37.0
Exit air temp. °C	29.0	30.2	30.4	30.4	30.4	30.2	30.0	30.0	30.0
Entering air temp. °F	81.5	81.2	81.5	81.2	80.7	80.7	80.0	80.0	79.2
Entering air % Rel. Humid.	89.5	90.5	91.5	91.5	91.5	91.5	91.5	91.5	90.5
Exit air % Rel. Humid.	100	100	100	100	100	100	100	100	100

Height of water in column = 27.8 inches

Flow Rate of Air = 0.222 $\frac{\text{lbs.}}{\text{hr.}}$

Table 6. Experimental Data (Sintered Glass Plug) (Continued)

Run 5

Time minutes	0	5	10	15	20	25	30
Water Temp. °C							
Bottom	43.1	42.5	42.1	41.5	41.0	40.6	40.2
Middle	431.	42.7	42.2	41.8	41.0	40.8	40.2
Top	43.1	42.6	42.1	41.6	41.0	40.6	40.2
Exit air temp. °C	29.5	29.6	29.8	29.8	29.9	29.9	29.8
Entering air temp. °F	81.7	81.2	81.2	81.2	81.2	81.2	80.1
Entering air % Rel.Humid.	91.5	91.5	91.5	91.5	91.5	91.5	91.5
Exit air % Rel. Humid.	100	100	100	100	100	100	100

Height of water in column = 29.2 inches

Flow Rate of Air = 0.151 $\frac{\text{lbs.}}{\text{hr.}}$

Run 6

Time minutes	0	5	10	15	20
Water Temp. °C					
Bottom	42.6	41.9	41.4	40.8	40.3
Middle	42.6	41.8	41.3	40.8	40.1
Top	42.6	41.9	41.4	40.8	40.2
Exit air temp. °C	29.3	29.2	29.2	29.1	29.0
Entering air temp. °F	81.7	82.5	81.7	81.2	80.0
Entering air % Rel.Humid.	91	91	91	91	91
Exit air % Rel. Humid.	100	100	100	100	100

Height of water in column = 26.8 inches

Flow Rate of Air = 0.151 $\frac{\text{lbs.}}{\text{hr.}}$

Table 7. Typical Bubble Size Distribution

Air Flow Rate = 0.0746 $\frac{\text{lbs.}}{\text{hr.}}$

Water Flow Rate = 0.208 $\frac{\text{lbs.}}{\text{min.}}$

Number of Bubbles m	Diameter cm. d
1	0.025
29	0.075
61	0.125
89	0.175
44	0.225
52	0.275
21	0.325
29	0.375
2	0.425
6	0.475
3	0.525
4	0.575

$\Sigma_m = 340$

Average $d_s = 0.244$ cm.

Average $d_v = 0.267$ cm.

BIBLIOGRAPHY

BIBLIOGRAPHY

1. Westwater, J. W., "The Boiling of Liquids", Scientific American, 190 (1954), pp. 64-68.

2. Perrott, G. St. J., and Kinney, S. P., "The Meaning and Microscopic Measurement of Average Particle Size", The Journal of the American Ceramic Society 6, (1923), pp. 417-439.

3. Ibid., pp. 417-439.

4. Gamson, Bernard, Thodos, George and Hougen, D. A., "Heat, Mass, and Momentum Transfer in the Flow of Gases Through Granular Solids", Transactions of the American Institute of Chemical Engineers 39, (1943), pp. 1-35.

5. McAdams, William H., Heat Transmission, First Edition. New York: McGraw-Hill Book Company, Inc., 1933. 383 pp.

6. Jakob, Max, Heat Transfer, Volume I. New York: John Wiley and Sons, Inc., 1949. 758 pp.

7. Peebles, F. N. and Garber, H. J., "Studies on the Motion of Gas Bubbles in Liquids", Chemical Engineering Progress 49, (1953), pp. 88-97.

8. Ingersoll, Leonard and Zobel, Otto, Mathematical Theory of Heat Conduction. New York: Ginn and Company, 1913. 200 pp.